

The Reticulon and Dp1/Yop1p Proteins Form Immobile Oligomers in the Tubular Endoplasmic Reticulum*[§]

Received for publication, February 6, 2008, and in revised form, March 31, 2008. Published, JBC Papers in Press, April 28, 2008, DOI 10.1074/jbc.M800986200

Yoko Shibata^{‡1}, Christiane Voss^{§1}, Julia M. Rist[‡], Junjie Hu[‡], Tom A. Rapoport^{‡2}, William A. Prinz^{§3,4}, and Gia K. Voeltz^{‡1,3,5}

From the [‡]Howard Hughes Medical Institute and Department of Cell Biology, Harvard Medical School, Boston, Massachusetts 02115, the [§]Laboratory of Cell Biochemistry and Biology, NIDDK, National Institutes of Health, Bethesda, Maryland 20892, and the [¶]Department of Molecular, Cellular, and Developmental Biology, University of Colorado, Boulder, Colorado 80309

We recently identified a class of membrane proteins, the reticulons and DP1/Yop1p, which shape the tubular endoplasmic reticulum (ER) in yeast and mammalian cells. These proteins are highly enriched in the tubular portions of the ER and virtually excluded from other regions. To understand how they promote tubule formation, we characterized their behavior in cellular membranes and addressed how their localization in the ER is determined. Using fluorescence recovery after photobleaching, we found that yeast Rtn1p and Yop1p are less mobile in the membrane than normal ER proteins. Sucrose gradient centrifugation and cross-linking analyses show that they form oligomers. Mutants of yeast Rtn1p, which no longer localize exclusively to the tubular ER or are even totally inactive in inducing ER tubules, are more mobile and oligomerize less extensively. The mammalian reticulons and DP1 are also relatively immobile and can form oligomers. The conserved reticulon homology domain that includes the two membrane-embedded segments is sufficient for the localization of the reticulons to the tubular ER, as well as for their diffusional immobility and oligomerization. Finally, ATP depletion in both yeast and mammalian cells further decreases the mobilities of the reticulons and DP1. We propose that oligomerization of the reticulons and DP1/Yop1p is important for both their localization to the tubular domains of the ER and for their ability to form tubules.

Most organelles have defined shapes that are evolutionarily conserved, but little is known about how the particular architecture of an organelle is formed and maintained. The structure

of the endoplasmic reticulum (ER)⁶ is one such example. The ER consists of the nuclear envelope, a double membrane surrounding the nucleus, and the peripheral ER. The peripheral ER is further morphologically divided into flat sheets that extend two-dimensionally, and tubules that have high curvature in their cross-section. In yeast, the bulk of the peripheral ER is maintained at the cell cortex with a small number of tubules connecting it to the nuclear envelope, whereas in higher eukaryotes the peripheral ER is found throughout the entire cytoplasm. Regardless of the spatial arrangement, however, these domains form a continuous membrane and luminal system (1–5).

Recently, we identified a class of integral membrane proteins, consisting of two distinct protein families, that structurally shape ER tubules (6). The first family is the reticulons, including four reticulon genes in mammals (*RTN1–4*), and two in yeast (*RTN1* and *RTN2*). The other family consists of the DP1/Yop1p proteins, which includes mammalian DP1 and its yeast homolog, Yop1p. Both families are found in all eukaryotes and are ubiquitously expressed. These proteins localize predominantly to the tubular ER and avoid the low curvature domains of the nuclear envelope and the peripheral sheets in a variety of eukaryotic species, including *Saccharomyces cerevisiae*, *Arabidopsis thaliana*, *Caenorhabditis elegans*, *Drosophila melanogaster*, and in *Xenopus* and mammals (6–11). The overexpression of certain isoforms of these proteins leads to long and unbranched tubules, whereas the deletion of the reticulons and *YOP1* in yeast leads to the loss of tubular ER (6). This yeast deletion mutant only exhibits a moderate growth defect, but the simultaneous depletion of both Rtn1p and Yop1p orthologs in *C. elegans* causes a 60% decrease in embryonic viability, suggesting that an intact, tubular ER is functionally important in higher eukaryotes (9).

The reticulons do not share any primary sequence homology with members of the DP1/Yop1p family. However, both families have a conserved domain of ~200 amino acids containing two long hydrophobic segments. Each hydrophobic segment seems to form a hairpin within the lipid bilayer so that all hydrophilic segments are found in the cytoplasm (6). The hydrophobic hairpins are proposed to form a “wedge” shape within the

* This work was supported, in whole or in part, by the National Institutes of Health NIDDK intramural research program (to W. A. P. and C. V.). The costs of publication of this article were defrayed in part by the payment of page charges. This article must therefore be hereby marked “advertisement” in accordance with 18 U.S.C. Section 1734 solely to indicate this fact.

[¶] Author's Choice—Final version full access.

[§] The on-line version of this article (available at <http://www.jbc.org>) contains supplemental Figs. S1–S5.

¹ Both authors contributed equally to this work.

² A Howard Hughes Medical Institutes Investigator.

³ Both authors contributed equally to this work.

⁴ To whom correspondence may be addressed: Laboratory of Cell Biochemistry and Biology, NIDDK, NIH, Bethesda, MD 20892. Tel.: 301-451-4592; Fax: 301-496-9431; E-mail: wprinz@helix.nih.gov.

⁵ Supported by a Searle Scholar Award. To whom correspondence may be addressed: Dept. of Molecular, Cellular, and Developmental Biology, University of Colorado, Boulder, CO 80309. Tel.: 303-492-3145; Fax: 303-492-7744; E-mail: gia.voeltz@colorado.edu.

⁶ The abbreviations used are: ER, endoplasmic reticulum; FRAP, fluorescence recovery after photobleaching; LBR, lamin B receptor; RHD, reticulon homology domain; GFP, green fluorescent protein; HA, hemagglutinin; PMSF, phenylmethylsulfonyl fluoride; EGS, ethylene glycobis(succinimidylsuccinate).

lipid bilayer, which would increase the surface area of the outer membrane leaflet to create the high curvature of ER tubules seen in their cross-section.

It is unlikely, however, that a simple wedge shape would be sufficient to induce tubules. The generation of high curvature by wedged-shape proteins may result in small spherical vesicles but is most likely insufficient to generate a cylindrical membrane that has almost no curvature along one axis. How this necessary anisotropy could be generated is unknown.

In the present report, we provide evidence that the reticulons and DP1/Yop1p form oligomers that are relatively immobile in the membrane. Our data suggest that the oligomerization of the reticulons and DP1/Yop1p plays an important role in the proper localization of these proteins in the ER and for tubule formation in living cells.

EXPERIMENTAL PROCEDURES

Yeast Strains and Constructs—The following yeast strains were used: BY4741 (*MATa his3Δ1 leu2Δ met15Δ ura3Δ*) and NDY257 (BY4741 *rtn1::kanMX4 rtn2::kanMX4 yop1::kanMX*) (6). Strains expressing GFP fusions to the chromosomal alleles of *YOP1* and *RTN1* were obtained from Invitrogen. The plasmid encoding Sec63-GFP (pJK59) has been previously described (12). To make the plasmid encoding Rtn1-GFP (pCV19), the *SEC63* portion of pJK59 was removed by digestion with XbaI and XhoI. The *RTN1* gene, including 400 bp upstream of the start site, was PCR-amplified from yeast chromosomal DNA and inserted into the same sites.

Mammalian Plasmid Constructs—HA-DP1 was described previously (6). HA-Rtn3c was cloned by PCR amplifying Rtn3c (NCBI accession number: BC036717) from mouse cDNA with primers containing an N-terminal HA tag and inserted into pcDNA3.1D (Invitrogen). For Rtn4a-GFP, human Rtn4a was PCR-amplified from Rtn4a-Myc (described in a previous study (6)) and ligated into the pAcGFP-N1 backbone (Clontech) using the XhoI and KpnI restriction sites at the 5' and 3' ends, respectively. For GFP-Rtn3c, Rtn3c was PCR-amplified from HA-Rtn3c and ligated into the pAcGFP-C1 backbone (Clontech) using the XhoI and EcoRI restriction sites. To clone GFP-Rtn4HD, the region encoding amino acids 961–1192 was PCR-amplified from human Rtn4a-Myc and inserted into pAcGFP-C1 using the XhoI/EcoRI restriction sites. GFP-DP1 was subcloned by PCR-amplifying mouse DP1 from HA-DP1 (described in a previous study (6)) and inserting into pAc-GFP C1 using SacI/BamHI restriction sites. For GFP-Climp63, Climp63 was PCR-amplified from mouse cDNA and cloned into pAcGFP-C1 using the XhoI/EcoRI sites. Climp63Δlum-GFP was cloned by PCR amplifying the region encoding amino acids 1–115 (as described in (13)) from GFP-Climp63 and inserted into pAcGFP-N1 using XhoI/EcoRI restriction sites. LBR-GFP was PCR-amplified from plasmid containing human LBR (14) and cloned into pAcGFP-N1 using the XhoI/BamHI restriction sites. For GFP-Sec61β, human Sec61β was PCR-amplified from the pcDNA3.1/GFP-Sec61β construct described previously (6), and inserted into pAcGFP-C1 using the BglII/EcoRI restriction sites. RFP-Sec61β was subcloned from GFP-Sec61β using the same restriction sites as above and

inserted into an mRFP1 vector (pEGFP-C1 vector backbone where pEGFP has been replaced with mRFP1).

Microscopy of Yeast—Yeast strains were grown in synthetic complete medium (0.67% yeast nitrogen base and 2% glucose) and imaged live at room temperature using an Olympus BX61 microscope, UPlanApo 100×/1.35 lens, QImaging Retiga EX camera, and IPLabs version 3.6.4 software.

Screen for Mutations in Yeast *RTN1* That Affect Localization—Error-prone PCR on *RTN1* was performed using the GeneMorphII Random Mutagenesis Kit (Stratagene). The product of this reaction and pJK59 cut with XbaI and XhoI were used to transform wild-type yeast. Transformants were visually screened for those that showed perinuclear GFP localization.

Tissue Culture, Indirect Immunofluorescence, and Confocal Microscopy of COS-7 Cells—Cells were grown at 37 °C with 5% CO₂ in Dulbecco's modified Eagle's medium containing 10% fetal bovine serum and subcultured every 2–3 days. Transfection of DNA into cells was performed using Lipofectamine 2000 (Invitrogen). After 5 h of transfection, cells were split onto acid-washed No. 1 coverslips and allowed to spread for an additional 24–36 h before being processed for indirect immunofluorescence.

For immunofluorescence, transfected cells were fixed in PBS containing 4% paraformaldehyde (Electron Microscopy Sciences) for 15 min, washed twice, and permeabilized in 0.1% Triton X-100 (Pierce) in PBS for 5–15 min. Cells were washed twice again and then probed with primary antibodies for 45 min in PBS containing 1% calf serum, at the following concentrations: rat anti-HA antibody (Roche Applied Science) at 1:200 dilution; mouse anti-αtubulin (Sigma) at 1:500 dilution; and rabbit anti-calreticulin antibody (Abcam) at 1:500 dilution. Cells were washed three times in PBS, and then incubated with various fluorophore-conjugated secondary antibodies for an additional 45 min (Alexafluor 488 or 555 anti-mouse at 1:250 dilution, Alexafluor 647 anti-rabbit 1:500 dilution, and Alexafluor 488 anti-rat 1:200 dilution (all from Invitrogen)). Cells were then washed and mounted onto slides using Fluoromount-G mounting medium (Southern Biotech).

All imaging for indirect immunofluorescence was captured using a Yokogawa spinning disk confocal on a Nikon TE2000U inverted microscope with a 100× Plan Apo numerical aperture 1.4 objective lens, and acquired with a Hamamatsu ORCA ER cooled charge-coupled device camera using MetaMorph 7.0 software. For image presentation, brightness and contrast were adjusted across the entire image using Adobe Photoshop 7.0, and images were converted from 12 to 8 bits.

Transmission Electron Microscopy—COS-7 cells expressing GFP-Rtn4HD were sorted in a MoFlo cell sorter (Cytomation). The resulting cell pellet was fixed for 1 h in a mixture of 2.5% glutaraldehyde and 2% paraformaldehyde in 0.1 M sodium cacodylate buffer (pH 7.4), washed in 0.1 M cacodylate buffer, and postfixated with a mixture of 1% OsO₄ and 1.5% KFeCN₆ for 30 min. The pellet was then washed in water and stained in 1% aqueous uranyl acetate for 30 min followed by dehydration in grades of alcohol (50%, 70%, and 95%, 2 × 100%). Next, the pellet was infiltrated in a 1:1 mixture of propylene oxide and

Reticulons and DP1/Yop1p Oligomerize in ER

TAAB Peon (Maria Canada Inc.) for 2 h, placed in pure TAAB Epon in a silicon-embedding mold, and polymerized at 65 °C for 48 h. Ultrathin sections (~60–80 nm) were cut on a Reichert Ultracut-S microtome, placed onto copper grids, and stained with 0.2% lead citrate. Specimens were examined on a Tecnai G Spirit BioTWIN transmission electron microscope, and images were acquired with a 2k AMT charge-coupled device camera.

Fluorescence Recovery after Photobleaching—Transfected COS-7 cells were imaged in phenol red-free HyQ DME (HyClone) supplemented with 25 mM Hepes, pH 7.4, and 1% fetal bovine serum. FRAP experiments were conducted on a Zeiss LSM 510 NLO laser scanning inverted microscope using a Plan-Neofluor 100×/1.3 oil objective with argon laser line 488 nm (optical slices <1.2 mm for COS-7 and 4.2 μm for yeast). Mammalian cell experiments were done at 37 °C using an objective heater (Biopetechs) and an enclosed stage incubator (Zeiss). LSM 510 software version 3.2 was used for image acquisition and analysis. Magnification, laser power, and detector gains were identical across samples.

For all mammalian experiments, COS-7 cells were treated with 0.5 μM nocodazole, and all data were collected during the first 5–30 min of nocodazole addition. For photobleaching all constructs, except for LBR-GFP, the tubular ER was magnified using the 3× zoom function so that individual tubules could be seen clearly. For LBR-GFP, the microscope was focused onto the bottom of the nuclear envelope. Images taken for 5-s pre-bleaching, whereupon a region of interest of 65 × 65 pixels was photobleached at 100% laser power. After the photobleaching, images were taken at 1-s intervals for 75–300 s. Yeast cells were treated similarly except that the region of interest was 17 × 17 pixels, and images were taken every 2–4 s at room temperature.

Raw data were quantitated using Zeiss LSM510Meta software. For analysis, the fluorescence intensity of three regions of interest was measured: the photobleached region (PR), a region outside of the cell to check for overall background fluorescence (BR), and a region within the cell that was not photobleached to check for overall photobleaching and fluorescence variation (CR), for the entire course of the experiment. Microsoft Excel was used to normalize the relative fluorescence intensity, *I*, for each individual FRAP experiment using Equation 1.

$$I = [(PR_t - BR_t)/(PR_{t_0} - BR_{t_0}) * 100] \\ \times [(100 - CR_t/CR_{t_0})/100 + 1] \quad (\text{Eq. 1})$$

For data presentation, the mean averages of the normalized data for each set of FRAP experiments were plotted using GraphPad Prism 5.0, and fluorescence recovery curves were shown for the first 80–140 s of each experiment. Estimated half-times of recovery and mobile fraction values were calculated using the standard Michaelis-Menten equation.

Sucrose Gradient Centrifugation—For yeast sucrose gradient analysis, crude membranes were isolated from yeast strains expressing GFP-fused proteins at endogenous levels as follows: 200 ml of culture were grown to OD ~1, pelleted and then resuspended in TKMG lysis buffer (50 mM Tris, pH 7.0, 150 mM KCl, 2 mM MgCl₂, 10% glycerol, 1 mM EDTA, 1 mM PMSF, 1 mM 4-(2-aminoethyl)benzenesulfonyl fluoride hydrochloride), flash

frozen in liquid nitrogen, and ground using a mortar and pestle. Cell debris was separated from the lysate by low speed centrifugation for 5 min at ~2,000 × *g*. Membranes were then pelleted by ultracentrifugation for 15 min at 100,000 × *g* and solubilized in 200 μl of TKMG buffer containing 1% digitonin. Solubilized lysate was centrifuged for 10 min at 12,000 × *g* to separate out any remaining cell debris. 100-μl of lysate were run on 5–30% w/v sucrose gradients for 4 h at 166,000 × *g* at 25 °C on a Beckman TLS55 rotor. Twenty gradient fractions were collected from top to bottom and analyzed by SDS-PAGE and immunoblotting with anti-GFP antibody (Roche Applied Science). 50 mg of apoferritin, catalase, and aldolase was used as molecular weight standards.

Xenopus washed membrane fractions were prepared in MWB (50 mM Hepes, pH 7.5, 2.5 mM MgCl₂, 250 mM sucrose, and 150 mM potassium acetate) as previously described (6), incubated for 60 min at 25 °C in MWB containing 200 mM KCl and 0.5 mM GTP, and then solubilized for 30 min at 25 °C with either 2% Nonidet P-40 or 1.25% digitonin. Samples were pelleted for 15 min at 12,000 rpm, and the soluble fraction was loaded onto a 10–30% w/v sucrose gradient made with MWB containing 200 mM KCl, 0.1 mM GTP, and either 0.1% Nonidet P-40 or 0.1% digitonin, respectively. The sucrose gradient was centrifuged for 3 h, 45 min at 55,000 rpm. Sixteen gradient fractions were collected and analyzed by SDS-PAGE and immunoblotted with antibody against *Xenopus* Rtn4 (described in a previous study (6)).

For mammalian sucrose gradient analysis, COS-7 cells transiently transfected with HA-DP1 or GFP-Sec61β were harvested by scraping and then lysed and solubilized in HKME buffer (25 mM Hepes, pH 7.8, 150 mM potassium acetate, 2.5 mM magnesium acetate, 1 mM EDTA, and 2 mM PMSF) containing 1% digitonin for 1 h. The lysate was clarified by centrifugation at 10,000 × *g* for 10 min, and 100 μl of clarified lysate was sedimented on 5–30% w/v sucrose gradients under the same conditions as yeast. Fractions were analyzed by SDS-PAGE and immunoblotting with anti-HA antibody or anti-Sec61β antibody (described in a previous study (15)).

Chemical Cross-linking Experiments—Yeast crude membrane fractions were resuspended in buffer containing 50 mM Hepes, pH 7.0, 150 mM KCl, and 1 mM PMSF. Ethylene glycol bis(succinimidylsuccinate) (EGS, Pierce), was dissolved in anhydrous DMSO and diluted to the desired concentration. 1 μl of EGS was added into every 20 μl of protein-containing sample for 30 min at room temperature. The reactions were quenched for 15 min with 2 μl of 1 M Tris, pH 7.5. Samples were analyzed on a 4–20% SDS-PAGE and immunoblotted using standard procedures with mouse anti-His or rat anti-HA antibody conjugated to peroxidase (Sigma).

For mammalian cross-linking experiments, transfected COS-7 cells were grown in a 10-cm plate to ~80% confluency and then lysed using a standard hypotonic lysis protocol. Briefly, cells were harvested in PBS, washed, incubated in hypotonic buffer (10 mM Hepes, pH 7.8, 10 mM potassium acetate, 1.5 mM magnesium acetate, 2 mM PMSF) for 10 min, and then passed through a 25-gauge syringe ten times. Nuclei and any remaining intact cells were separated from the lysate by centrifugation for 5 min at 3,000 × *g*, and the supernatant was then

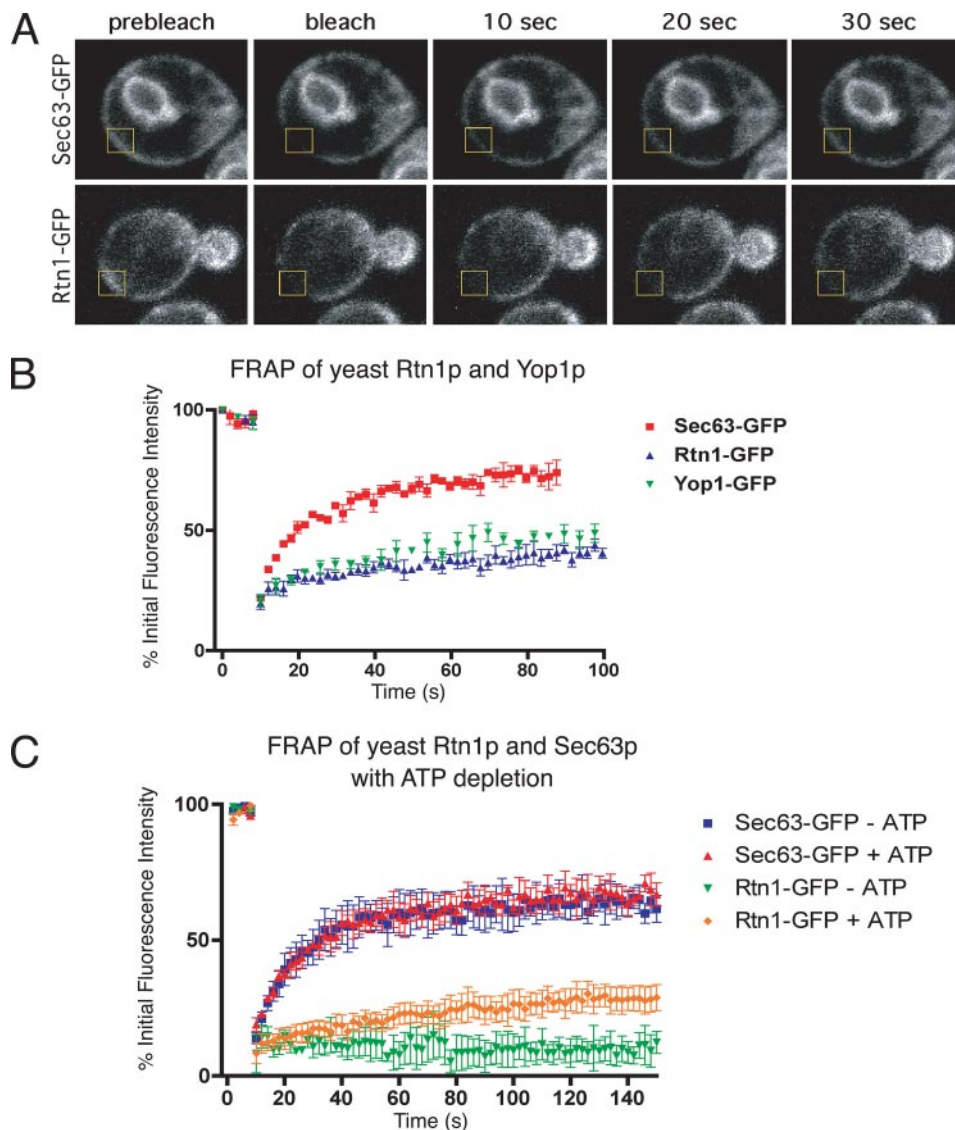


FIGURE 1. Rtn1p and Yop1p have slow diffusional mobility in the ER of yeast cells. *A*, typical FRAP of Sec63-GFP or Rtn1-GFP in *S. cerevisiae* cells expressed at endogenous levels. Images were taken before and then after the photobleach for the times indicated. The boxed region shows the area that was photobleached. *B*, fluorescence intensities normalized to prebleach values of FRAP analyses on yeast Sec63-GFP, Rtn1-GFP, and Yop1-GFP were plotted over time. Error bars indicate \pm S.E.; $n = 4$ cells. *C*, fluorescence intensities normalized to prebleach values plotted over time of FRAP analyses on yeast Rtn1p in ATP-depleted (green) or non-depleted (orange) cells, compared with that of Sec63p-GFP (ATP depleted in blue; non-depleted in red). Error bars indicate \pm S.E.; $n = 4$ cells.

centrifuged for 10 min at $100,000 \times g$ to pellet the membrane fraction. The membrane pellet was washed in HKM buffer (25 mM HEPES pH 7.8, 150 mM potassium acetate, 2.5 mM magnesium acetate, and 2 mM PMSF), repelleted at $100,000 \times g$, and resuspended to a final volume of $60 \mu\text{l}$ in HKM buffer. $10\text{-}\mu\text{l}$ membrane aliquots were used for each cross-linking reaction using the same conditions as above. Samples were analyzed on a 4–20% SDS-PAGE and immunoblotted using standard procedures with anti-HA antibody.

ATP Depletion Experiments—For yeast experiments, ATP was depleted by the addition of 10 mM 2-deoxy-D-glucose and 10 mM sodium azide (both from Sigma) for 2–5 min, and FRAP experiments were performed using the same parameters as described above. Similarly, for mammalian cell experiments, COS-7 cells were depleted of ATP as follows: trans-

fectected cells were washed twice in Opti-Mem serum-free media (Invitrogen) and then incubated with 50 mM 2-deoxy-D-glucose and 0.02% sodium azide in glucose-free imaging buffer (50 mM HEPES, pH 7.4, 150 mM potassium acetate, 2.5 mM magnesium acetate, and 1% fetal bovine serum). FRAP experiments were conducted in the same medium and completed within 5–30 min of treatment using the same parameters as above.

RESULTS

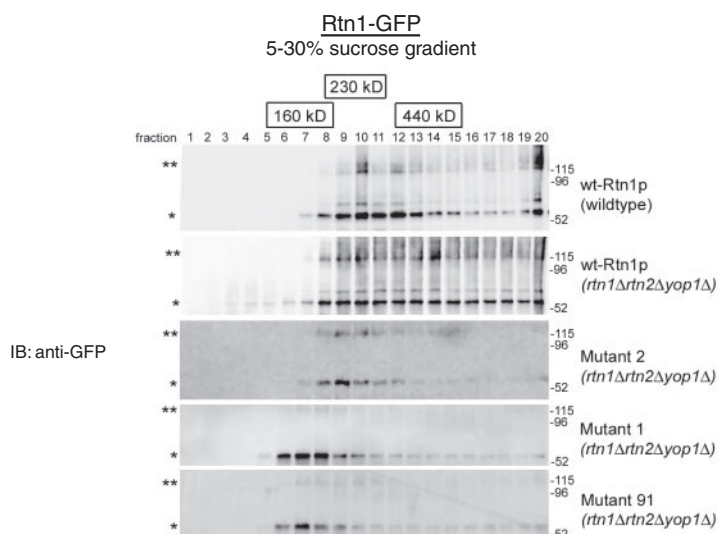
Yeast Rtn1p and Yop1p Are Immobile Proteins in the ER Membrane—The reticulons and DP1/Yop1p may promote tubule formation in the ER by assembling into structures that surround the membrane and deform it (16). We predicted that such structures might be immobile in the lipid bilayer. To test whether the reticulons and Yop1p differ in their diffusional mobility from normal ER membrane proteins, we used fluorescence recovery after photobleaching (FRAP). This technique determines the diffusional kinetics of integral membrane proteins in living cells (17, 18).

We conducted FRAP experiments in yeast cells expressing GFP fusions to Rtn1p or Yop1p. As a control, we analyzed Sec63-GFP, a 75-kDa resident ER protein with three transmembrane segments. Notably, all of these proteins were expressed under their endogenous promoters. A small portion of the cortical ER was photobleached, and

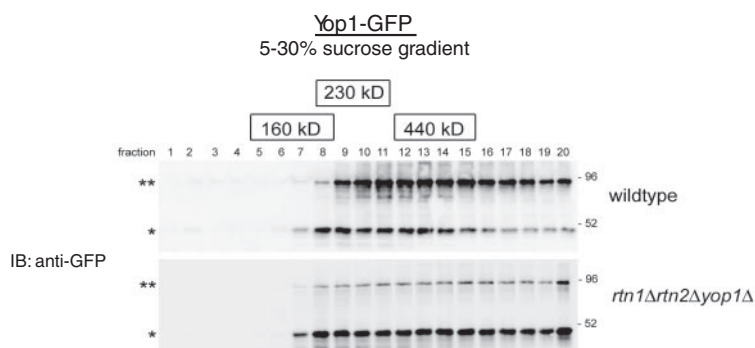
fluorescence recovery was measured over time (Fig. 1*A*). Rtn1p and Yop1p both displayed relatively slow and restricted diffusional properties compared with Sec63p (Fig. 1*B*). These FRAP data show that Rtn1p and Yop1p diffuse significantly more slowly in the membrane than normal ER proteins.

Rtn1p and Yop1p Form Oligomers in the Membrane—Rtn1p and Yop1p may diffuse slowly within membranes because they are tethered to the cytoskeleton or because they oligomerize (6, 19–21). We ruled out that low mobility is caused by association with actin filaments, the major cytoskeletal element responsible for yeast ER dynamics (12, 22), because no significant difference in mobility was seen in cells treated with latrunculin (data not shown). Therefore, we wondered if oligomerization of Rtn1p and Yop1p caused their low mobility in the ER membrane, because it had been previously shown that the reticulons and

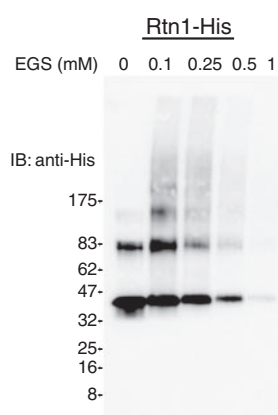
A



B



C



D

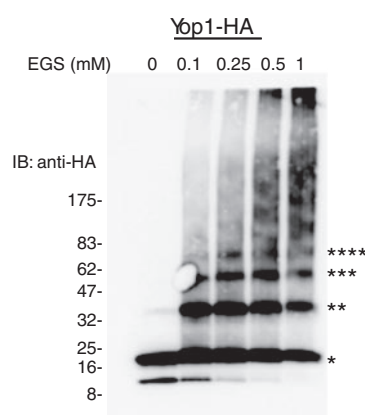


FIGURE 2. Yeast Rtn1p and Yop1p form homo-oligomers in the membrane. *A*, membranes isolated from wild-type or *rtn1Δrtn2Δyop1Δ* (NDY257) yeast cells expressing wild-type or mutant forms of Rtn1-GFP at endogenous levels were solubilized in 1% digitonin, fractionated by 5–30% w/v sucrose gradient centrifugation, and analyzed by SDS-PAGE and immunoblotting with anti-GFP antibody. Note that the mutant forms of Rtn1p have peak migrations at a smaller molecular weight than the wild-type protein. *B*, membranes isolated from wild-type or *rtn1Δrtn2Δyop1Δ* yeast cells expressing wild-type Yop1-GFP at endogenous levels were solubilized in 1% digitonin and were analyzed as in *A*. Molecular weight standards in the sucrose gradient are as indicated. *C*, isolated membranes of yeast cells expressing Rtn1-His were treated with increasing concentrations of EGS and analyzed on SDS-PAGE, and oligomers were visualized by immunoblotting with anti-His antibody. *D*, membranes of yeast cells expressing Yop1-HA were analyzed as in *C* and immunoblotted with anti-HA antibody. Asterisks, number of monomeric copies of the specified protein as seen by SDS-PAGE.

DP1/Yop1p can interact with themselves and with each other (6, 19–21).

Preliminary evidence for the idea that oligomerization of Rtn1p causes its slow diffusional mobility was obtained with cells depleted of ATP. Yeast cells expressing Rtn1-GFP were depleted of ATP with 10 mM 2-D-deoxyglucose and 10 mM sodium azide and subjected to FRAP analysis. Rtn1-GFP became essentially immobile, whereas the control membrane protein Sec63-GFP showed no significant change in diffusional mobility (Fig. 1C). The simplest interpretation of these results is that Rtn1p forms oligomers whose size increases in the absence of ATP, perhaps because ATP is required for the disassembly of the oligomers.

To provide more direct evidence for oligomerization, we used sucrose gradient centrifugation. Membranes purified from yeast cells expressing Rtn1-GFP at endogenous levels were solubilized in 1% digitonin. The detergent extracts were subjected to sucrose gradient centrifugation, and fractions were analyzed on SDS-PAGE and immunoblotting with GFP antibodies (Fig. 2*A*, top panel). A major band of the expected size was seen. A second band consistent in size with an SDS-resistant dimer was also observed, but its intensity varied in different experiments, perhaps because of slight differences in expression levels. The protein peaked at a molecular mass of ~300–350 kDa when compared with molecular weight marker proteins, indicating that these complexes may contain 4 or 5 monomers. In addition, some Rtn1p molecules were found in higher molecular weight complexes. When Rtn1-GFP was solubilized with the harsher detergent Nonidet P-40, it ran at a lower molecular weight (supplemental Fig. S1).

Similar results were obtained with Yop1-GFP, again expressed at endogenous levels. The majority of Yop1-GFP migrated in the density gradients at a size of ~300–400

kDa (Fig. 2B), indicating that this protein is present in a complex of a similar size to those containing Rtn1p. A prominent SDS-resistant dimer form was also seen. Both Rtn1-GFP and Yop1-GFP sedimented at a similar position when expressed in yeast cells lacking endogenous Rtn1p, Rtn2p, and Yop1p (Fig. 2, A and B). These data indicate that these proteins can form homo-oligomers. The relative amounts of Rtn1-GFP and Yop1-GFP in the higher molecular weight fractions in the *rtn1Δrtn2Δyop1Δ* cells were more prominent (Fig. 2A, top two panels, and Fig. 2B) than in wild-type cells, suggesting that these proteins may form larger complexes when they homo-oligomerize.

Next, we used chemical cross-linking to determine the oligomeric state of Rtn1p and Yop1p in intact membranes. Membranes were isolated from yeast cells expressing Rtn1-His or Yop1-HA, treated with EGS, a bifunctional cross-linker, and then analyzed by SDS-PAGE and immunoblotting using His or HA antibodies. With increasing EGS concentrations, a "ladder" of cross-linked bands became apparent whose molecular sizes are consistent with homo-oligomers of Rtn1-His or Yop1-HA (Fig. 2, C and D). Up to four cross-linked monomers could be easily distinguished with SDS-PAGE, consistent with the size estimate of the major protein population in our sucrose gradient centrifugation experiments. In addition, a higher molecular weight smear can also be seen, suggesting that larger complexes can also form. Together, these data suggest that Rtn1p and Yop1p can form homo-oligomeric complexes containing at least four and probably more monomers. The observed oligomerization could explain their slow diffusion in the ER membrane.

Mutations in Rtn1p That Affect Its Localization in Vivo Have Oligomerization Defects—We wished to determine whether the exclusive localization of Rtn1p to the tubular ER correlates with its ability to form oligomers. We reasoned that mutants in Rtn1p that have lost their specific localization would have defects in oligomerization. Thus, we first screened for mutations in yeast Rtn1-GFP that cause it to localize not only to the peripheral tubular ER but also to the nuclear envelope. The *RTN1* portion of the *RTN1*-GFP fusion was mutated by error-prone PCR and introduced into a low copy plasmid by homologous recombination. Approximately 2000 transformants were visually screened, and two independent mutants, Mutant 1 and Mutant 2, were isolated that showed nuclear envelope staining in addition to cortical ER localization (Fig. 3E). The point mutations in both mutants are indicated in Fig. 3A. Both mutants contained several amino acid changes. There were five mutations in Mutant 1, three of which are localized to the intervening region. No single mutation was the cause of this relocalization, suggesting a synergistic relationship amongst several mutations. For Mutant 2, however, site-directed mutagenesis showed that the lysine to isoleucine mutation in the first membrane-embedded region, K48I, is responsible for the mislocalization. Both mutant proteins were relatively stable and localized to the membrane (supplemental Fig. S2).

Next, we determined whether these mutant proteins had a decreased ability to form immobile oligomers. When analyzed using FRAP, Mutant 1 and 2 were significantly more mobile than wild-type Rtn1-GFP (Fig. 3, B and C). Interestingly, the mobility of the Rtn1p mutants was not affected by ATP depletion

(data not shown), in contrast to that of the wild-type protein (see Fig. 1C). The mutants also appeared to have defects in oligomerization in sucrose gradient centrifugation experiments, because they migrated at lower molecular weight compared with the wild-type protein (Fig. 2A, third and fourth panels). Because these proteins are associated with a detergent micelle, it is unclear whether they were completely monomeric. These findings suggest that oligomerization is indeed responsible for the exclusive localization of Rtn1p in the tubular ER and for its immobility in the membrane.

We noticed that the Rtn1p mutants were not entirely non-functional: when expressed on a CEN plasmid in a *rtn1Δrtn2Δyop1Δ* triple knock-out mutant (which has only sheet-like ER), they were able to regenerate the tubular ER similar wild-type Rtn1p (Fig. 3E, middle three panels). One possible explanation is that these mutants still maintain a low level of oligomerization. Indeed, cross-linking with a bifunctional reagent still produced a ladder of Rtn1p bands (data not shown). By combining the mutations in Mutants 1 and 2, we were able to generate a mutant (Mutant 91) that no longer restored the tubular ER morphology when expressed in *rtn1Δrtn2Δyop1Δ* cells (Fig. 3E, far right panels). However, while Mutant 91 diffused rapidly in the membrane (Fig. 3D) and migrated at a lower molecular weight in sucrose gradient centrifugation (Fig. 2A, bottom panel), it still seemed to oligomerize, as seen in cross-linking experiments (not shown). Thus, oligomerization may not be the only feature required for the ability of Rtn1p to form tubules.

Mammalian Rtn4a and DP1 Are Also Immobile in the Membrane—We next determined whether the mammalian homologs of yeast Rtn1p and Yop1p also oligomerize and diffuse slowly in the ER membrane. We performed analogous FRAP experiments on a number of mammalian GFP-fused ER proteins expressed in COS-7 cells (indicated in Fig. 4).

We previously had found that mammalian Myc-tagged Rtn4a and hemagglutinin (HA)-tagged DP1 localize exclusively to the tubular ER (6). The same localization was also seen when these proteins were tagged with monomeric GFP. GFP-DP1 also formed perinuclear aggregates in cells highly expressing this protein (data not shown). At moderate expression levels, Rtn4a-GFP and GFP-DP1 localized to the tubular ER and were absent from the NE and peripheral sheets in COS-7 cells (Fig. 5, A and B). In contrast, RFP-fused Sec61β (RFP-Sec61β), a normal resident ER membrane protein, was seen in all ER domains.

To analyze the diffusional mobility of mammalian Rtn4a-GFP and GFP-DP1 in the tubular ER by FRAP, we first selected a small portion of the ER in the periphery of a cell, where a single layer of tubular network can be visualized. In our initial FRAP experiments, we found that the ER tubules were highly dynamic, often growing into the photobleached region within seconds (data not shown). The fluorescence recovery seen was thus not that of protein diffusion in the membrane, but of ER tubule movement itself. To remedy this and effectively "freeze" the microtubule-dependent ER tubule movement (23), transfected cells were first treated with 0.5 μM nocodazole, a concentration that inhibited microtubule dynamics and partially depolymerized the cytoskeleton. All subsequent FRAP experiments

A

```

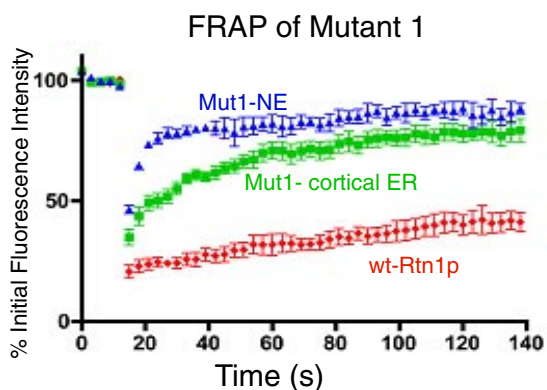
MSASAQHSQAQQQQQKSCNCDLLWRNPVQTGKYFGGSLALLILKKNVNLITFFLKV
AYTILFTTGSIEFVSKLFLGQGLITKYGPKECPNIAGFIKPHIDEALKQLPVFQAHIRKTVF
AQVPKHTFKTAVALLFLHKKFFSWFSIWTVFVADIFTFPLPVIYHSYKHEIDATVAQGVEI
SKQKTQEFSSQMACEKTKPYLDKVESKLGPISNLVKSKTAPVSSSTAGPQTASTSKLAADV
PLEPESKAYTSSAQVMPEVPQHEPSTTQEFNVDELSEELKKSTKNLQNELEKNNA Stop
    
```

Mutant 1: H7Y, T127I, I137P, H138R, N277Y

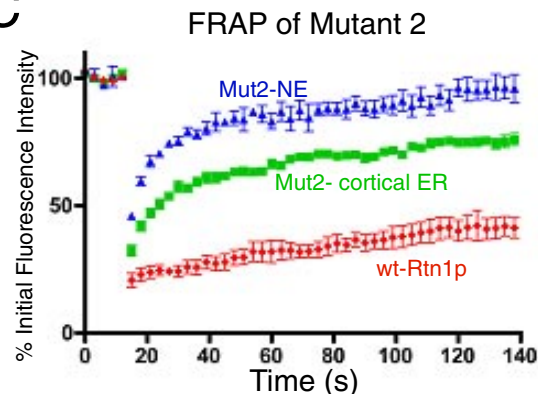
Mutant 2: K48I*, P87L, T157S

Mutant 91: H7Y, K48I, T127I, I37P, N277Y

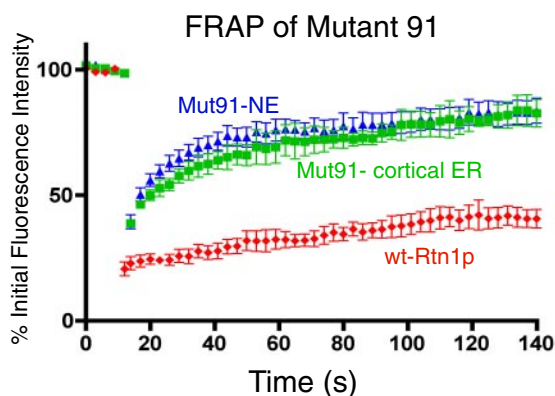
B



C



D



E

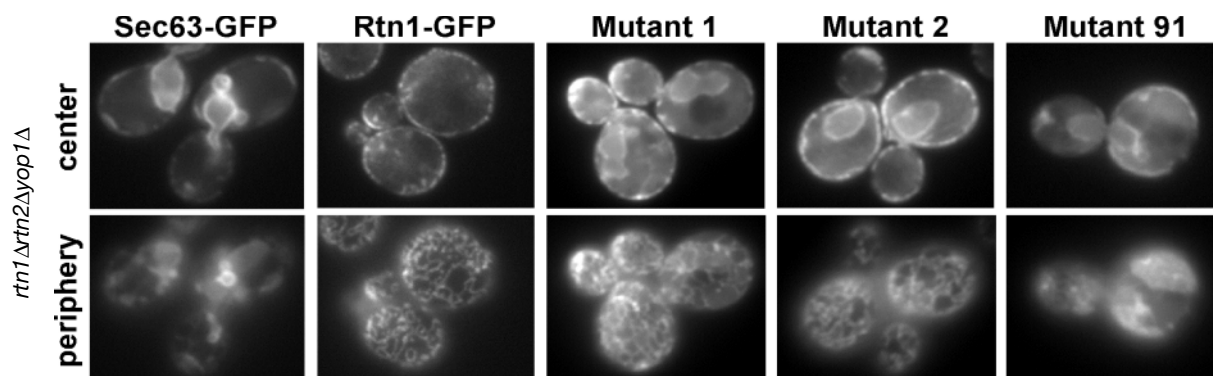


FIGURE 3. A yeast Rtn1p mutant with defects in localization and oligomerization also cannot shape tubules *in vivo*. A, mutations in Rtn1 Mutant 1, Mutant 2, and Mutant 91 that affect the ability of the protein to localize exclusively to the tubular ER. The residues altered in Mutant 1 are shown in blue, and those in Mutant 2 are shown in green. K48I is responsible for the altered localization of Mutant 2. The combined mutations of Mutant 91 are indicated in purple. The two membrane-embedded regions are indicated in red. B–D, fluorescence intensities normalized to prebleach values plotted over time from FRAP analyses of Rtn1-GFP Mutant 1 (B), Mutant 2 (C), or Mutant 91 (D) expressed in wild-type *S. cerevisiae* cells. Error bars indicate \pm S.E., $n = 4–8$ cells. E, the indicated GFP fusions were constitutively expressed under their endogenous promoters in *rtn1Δrtn2Δyop1Δ* cells. The ER was visualized by focusing on either the center or periphery of the cell. Note that wild-type, Mutant 1, and Mutant 2 Rtn1-GFP restore tubular ER structure, whereas Mutant 91 and the control protein Sec63-GFP do not.

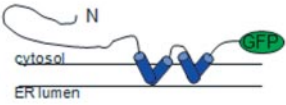
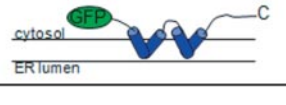
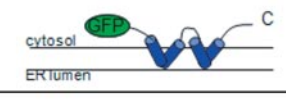
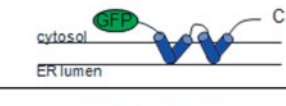

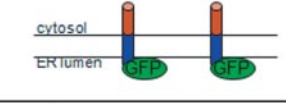

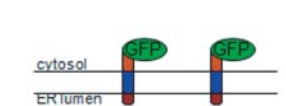
Name	Construct Topology	Known Mobility
Rtn4a-GFP		?
GFP-DP1		?
GFP-Rtn4HD		?
GFP-Rtn3c		?
GFP-Climp63		Immobile <i>Klopfenstein et al., 2001.</i>
Climp63Δlum-GFP		Mobile <i>Klopfenstein et al., 2001.</i>
LBR-GFP		Immobile <i>Ellenberg et al., 1997.</i>
GFP-Sec61β		Mobile <i>Rolls et al., 1999.</i>

FIGURE 4. Mammalian GFP-fused membrane proteins and their known lateral mobilities used for FRAP analysis.

were conducted in the presence of nocodazole and performed within 5–30 min upon addition of the drug.

Upon photobleaching, both Rtn4a-GFP and GFP-DP1 diffused relatively slowly into the bleached area, much more slowly than the control membrane protein, GFP-Sec61β (Fig. 5C). Quantitating the fluorescence intensities normalized to prebleach values showed that the half-times of recovery were ~3- to 4-fold slower than that of the control membrane protein GFP-Sec61β (Fig. 5, D and E). Moreover, although GFP-Sec61β showed almost maximal recovery to prebleach levels, GFP-DP1 and Rtn4a-GFP only recovered to a maximum of ~50 and ~60%, respectively.

The diffusional kinetics of Rtn4a-GFP and GFP-DP1 were similar to that of lamin B receptor (LBR), a protein that has restricted mobility due to its association with the nuclear lamina (Fig. 5, D and E) (24). The mobilities of both Rtn4a and DP1 were also similar to that of another relatively immobile ER protein, Climp-63 (Fig. 5F). GFP-Climp63 diffuses slowly because it oligomerizes extensively with itself via its large coiled-coil

luminal domain (13). A mutant Climp-63 lacking this luminal domain, GFP-Climp63Δlum, diffuses rapidly (13) with similar kinetics to that of GFP-Sec61β (Fig. 5G). These results indicate that both Rtn4a-GFP and GFP-DP1 have slow and restricted diffusional mobility within the membrane, consistent with the FRAP data obtained in yeast.

The Reticulon Homology Domain Is Sufficient for Localization to Tubules and for Diffusional Immobility—All reticulons possess a reticulon homology domain (RHD), which contains the two membrane-embedded hairpins, but the length and sequence of the N terminus differ greatly among different mammalian isoforms (25). To test whether the conserved RHD is sufficient to localize the reticulons to ER tubules, we deleted the N-terminal region from Rtn4a and expressed the remaining segment (Rtn4HD) as a GFP fusion in COS-7 cells. Like the full-length Rtn4a protein, GFP-Rtn4HD localized to tubules, but was absent from the peripheral ER sheets and the nuclear envelope (Fig. 6A). An exclusively tubular ER localization was also seen with GFP-fused Rtn3c, another reticulon isoform expressed from a different gene, which also consists of only the RHD (Fig. 6B). These results indicate that the conserved RHD mediates the exclusive tubular localization of the reticulons in mammalian cells.

Next, we tested whether the RHD is also sufficient for the slow lateral mobility of the reticulons. FRAP experiments were done on the two reticulon isoforms, GFP-Rtn4HD and GFP-Rtn3c. For these experiments, we selected cells expressing these proteins only at moderate levels, because these proteins were found enriched in aberrant ribbon- or globule-like membrane structures in highly expressing cells. These structures did not colocalize with endogenous ER or Golgi markers and were reminiscent of crystalloid membranes in transmission electron microscopy (supplemental Fig. S3 and data not shown).

FRAP analyses showed that both GFP-Rtn4HD and GFP-Rtn3c diffuse slowly compared with GFP-Sec61β and have similar diffusional kinetics to LBR-GFP (Fig. 6, C–E). These results support a model in which the highly conserved RHD mediates both their tubular localization and their slow diffusional properties. This is consistent with our results on yeast Rtn1p, which also contains little more than the RHD.

Reticulons and DP1 Oligomerize in Higher Eukaryotes—As in yeast, we obtained initial evidence for oligomerization of the reticulons and DP1 by performing FRAP analysis on cells depleted of ATP. COS-7 cells expressing the GFP-fused proteins were treated with 50 mM 2-D-deoxyglucose and 0.02% sodium azide, and FRAP experiments were conducted in the first 30 min of treatment. ATP depletion did not have gross effects on tubular ER morphology (data not shown), but it decreased the mobility of Rtn3c, Rtn4HD, and DP1 (Fig. 7A and supplemental Fig. S4). In contrast, the mobility of the control membrane protein, GFP-Sec61β, remained unchanged (Fig. 7B). These results suggest that the reticulons and DP1 form oligomers, the size of which is regulated by ATP.

Direct evidence for oligomerization was obtained by sucrose gradient centrifugation and chemical cross-linking. We first tested the oligomerization of Rtn4a and Rtn4b in *Xenopus* oocyte membranes. The membranes were solubilized in either digitonin or Nonidet P-40, and the detergent extracts were sub-

Reticulons and DP1/Yop1p Oligomerize in ER

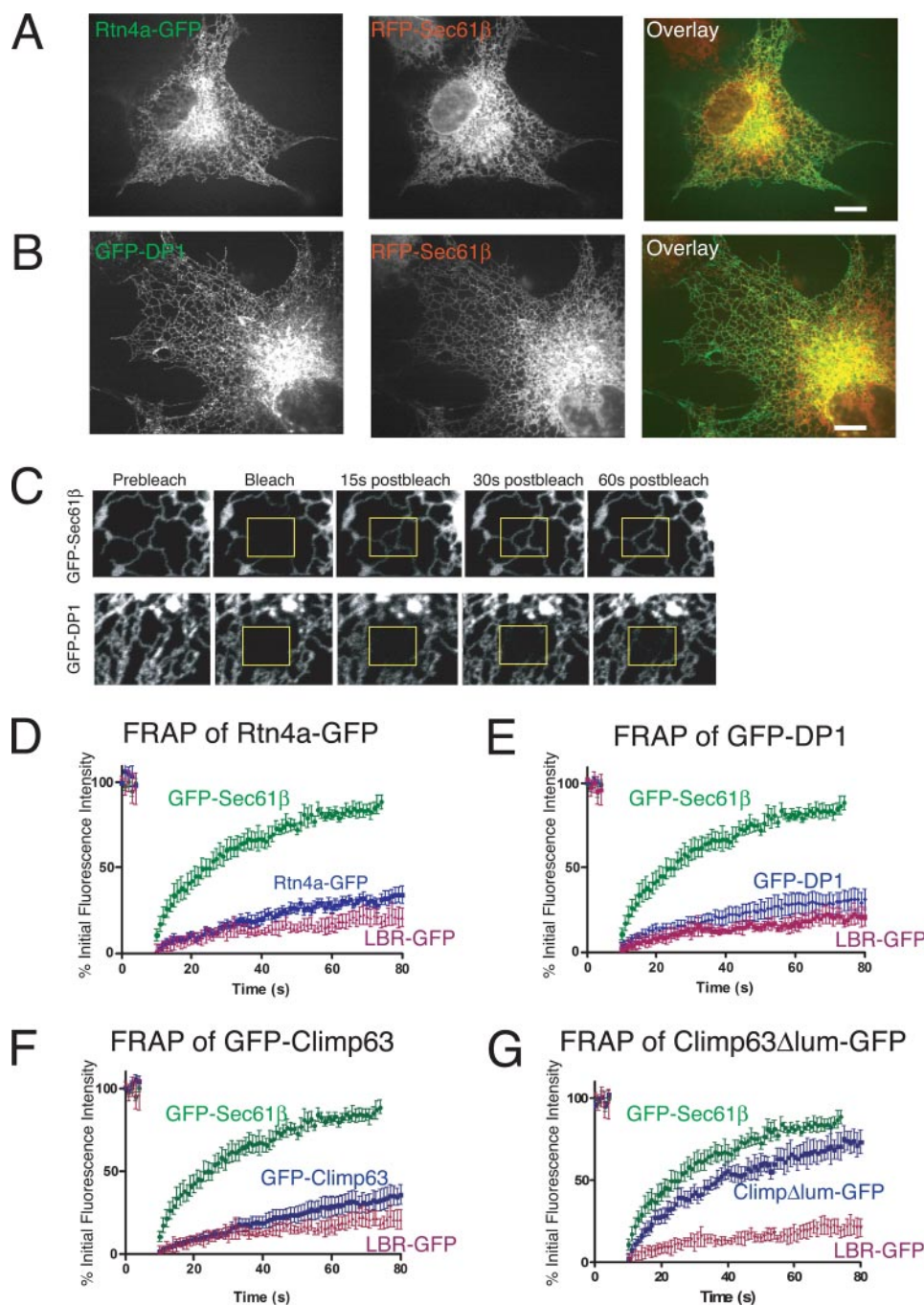


FIGURE 5. Mammalian Rtn4a-GFP and GFP-DP1 have slow, restricted lateral mobilities in ER tubules. *A* and *B*, Rtn4a-GFP and GFP-DP1 (both in *green*) expressed in COS-7 cells localize only to the tubular ER, whereas a normal resident ER membrane protein, RFP-Sec61 β (*red*) localizes to all ER subdomains, including the nuclear envelope and peripheral sheets. *C*, fluorescence recovery of GFP-DP1 compared with the control membrane protein GFP-Sec61 β . Images were taken before and then after the photobleach for the times indicated. The boxed region shows the area that was photobleached. *D*, quantitation of FRAP analyses of Rtn4a-GFP (*blue*; $n = 7$ cells) compared with GFP-Sec61 β (*green*; $n = 6$) and LBR-GFP (*red*; $n = 3$), where the average fluorescence intensity normalized to prebleach values was plotted over time. *E*, quantitation of FRAP analyses of GFP-DP1 (*blue*; $n = 9$) compared with GFP-Sec61 β (*green*) and LBR-GFP (*red*). *F*, quantitation of FRAP analyses of GFP-Climp63, an ER membrane protein known to be immobile through homo-oligomerization (*blue*; $n = 6$), compared with GFP-Sec61 β (*green*) and LBR-GFP (*red*). *G*, quantitation of FRAP analyses of Climp63 Δ lum-GFP, a mutant form of Climp63 lacking its luminal homo-oligomerization domain (*blue*; $n = 5$), compared with GFP-Sec61 β (*green*) and LBR-GFP (*red*). All error bars indicate \pm S.E.

jected to sucrose gradient centrifugation (Fig. 7C). The size difference between the two detergents suggests that both reticulons form oligomers. We also found that digitonin-solubilized HA-DP1 expressed in COS-7 cells migrated in sucrose gradient

centrifugation at a molecular weight consistent in size with larger multimeric complexes (supplemental Fig. S4). Digitonin efficiently solubilized membrane proteins, as GFP-Sec61 β monomers sedimented at lower molecular weight fractions (supplemental Fig. S4).

Cross-linking experiments further confirmed that these proteins oligomerize in membranes. Membranes of COS-7 cells transiently transfected with HA-Rtn3c were isolated, treated with increasing concentrations of the bifunctional cross-linker EGS, and analyzed by SDS-PAGE and immunoblotting. As in yeast, a multimeric ladder was observed, with the step size being consistent with homo-oligomers (Fig. 7D). These data indicate that the RHD of the reticulons is sufficient for their ability to oligomerize. Homo-oligomer formation was also observed when HA-DP1 was cross-linked (Fig. 7E). Taken together, these results indicate that the reticulons and DP1/Yop1p form oligomers in yeast and mammalian cells, suggesting that they do so in all eukaryotic cells.

Mammalian Reticulons or DP1 Can Stabilize ER Tubules in the Absence of Microtubules—We hypothesized that, if reticulum proteins form oligomeric structures that directly shape and stabilize the tubular ER, then overexpressing these proteins might stabilize the tubular shape of membranes *in vivo* under conditions where the tubular ER is normally disrupted. Prolonged depolymerization of microtubules is known to cause peripheral ER tubules to retract to the cell center, resulting in unstructured, cisternal ER (26). When COS-7 cells expressing the control membrane protein GFP-Sec61 β were treated with 1 mM nocodazole for 30 min to completely depolymerize all dynamic microtubules, the tubular ER converted into mostly sheet-like structures (Fig. 8A). However, when we subjected COS-7 cells overexpressing GFP-Rtn3c to the same treatment, large parts of the tubular ER remained intact, with many tubules connected by three-way junctions present (Fig.

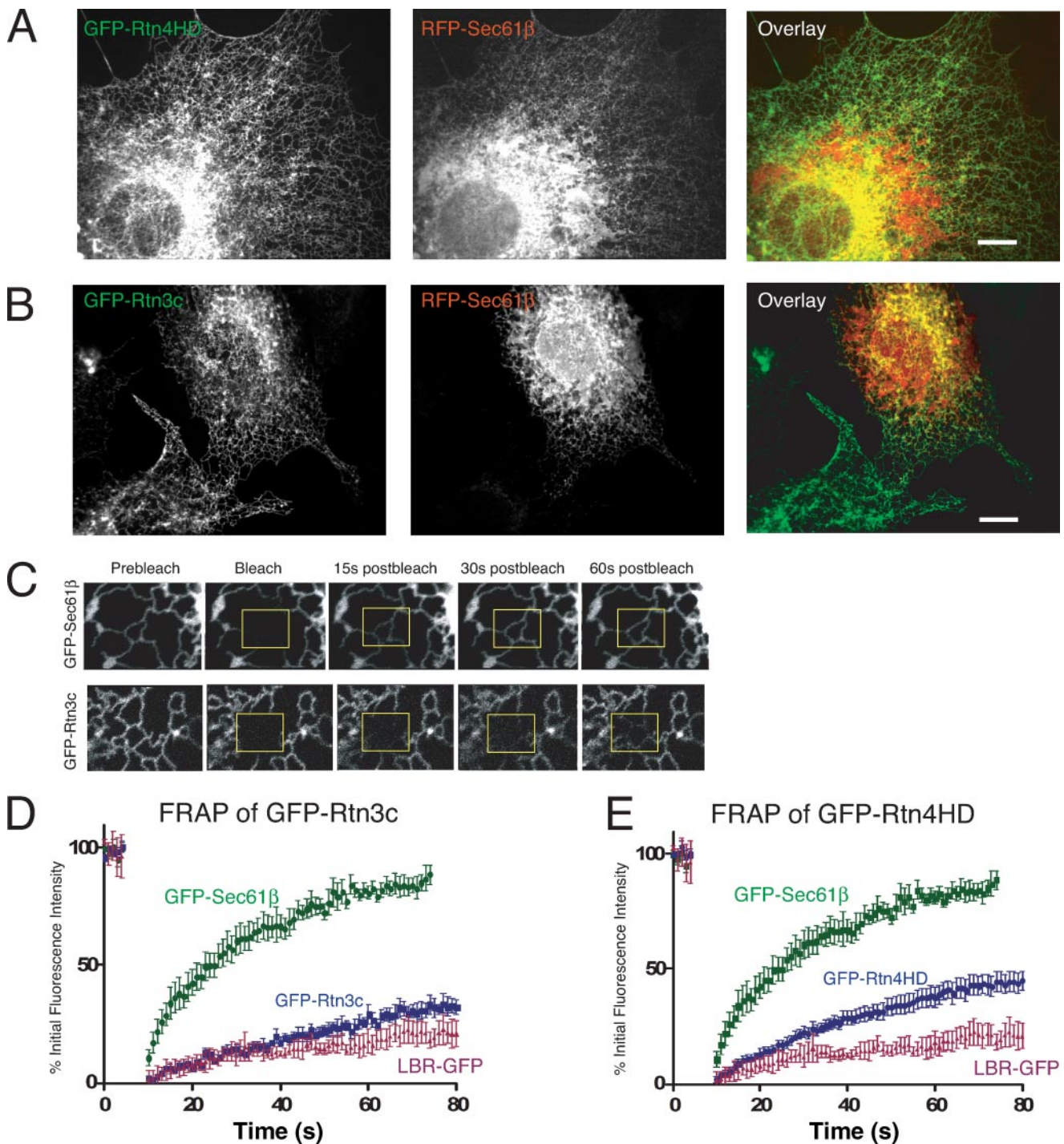


FIGURE 6. The conserved RHD is sufficient for the diffusional immobility of the mammalian reticulons. *A* and *B*, exclusive tubular ER localization of GFP-Rtn4HD and GFP-Rtn3c (both in green), two reticulon isoforms containing only the conserved reticulon homology domain, compared with the general membrane protein RFP-Sec61 β (red) when expressed in COS-7 cells. *C*, typical FRAP experiments performed in COS-7 cells comparing the fluorescence recovery of GFP-Rtn3c to GFP-Sec61 β illustrates that reticulons containing only the RHD is relatively immobile. Images were taken before and then after the photobleach for the times indicated. The boxed region shows the area that was photobleached. *D*, quantitation of FRAP analyses of GFP-Rtn3c (blue; $n = 6$) compared with GFP-Sec61 β (green) and LBR-GFP (red), where fluorescence intensities normalized to prebleach values were plotted over time. *E*, quantitation of FRAP analyses of GFP-Rtn4HD (blue; $n = 14$), compared with GFP-Sec61 β (green) and LBR-GFP (red). All error bars indicate \pm S.E.

8B). Some of the protein also accumulated bright punctae that colocalized with other endogenous ER markers (data not shown). Similar results were seen in cells overexpressing Rtn4a, Rtn4HD, or DP1 (data not shown). Thus, it appears that increased levels of the reticulons or DP1 can stabilize the tubular ER in the absence of the cytoskeletal network in

mammalian cells, consistent with their proposed role in structurally stabilizing ER tubules.

DISCUSSION

Here we demonstrate that the reticulons and DP1/Yop1p diffuse only slowly in the membrane in both yeast and mamma-

Reticulons and DP1/Yop1p Oligomerize in ER

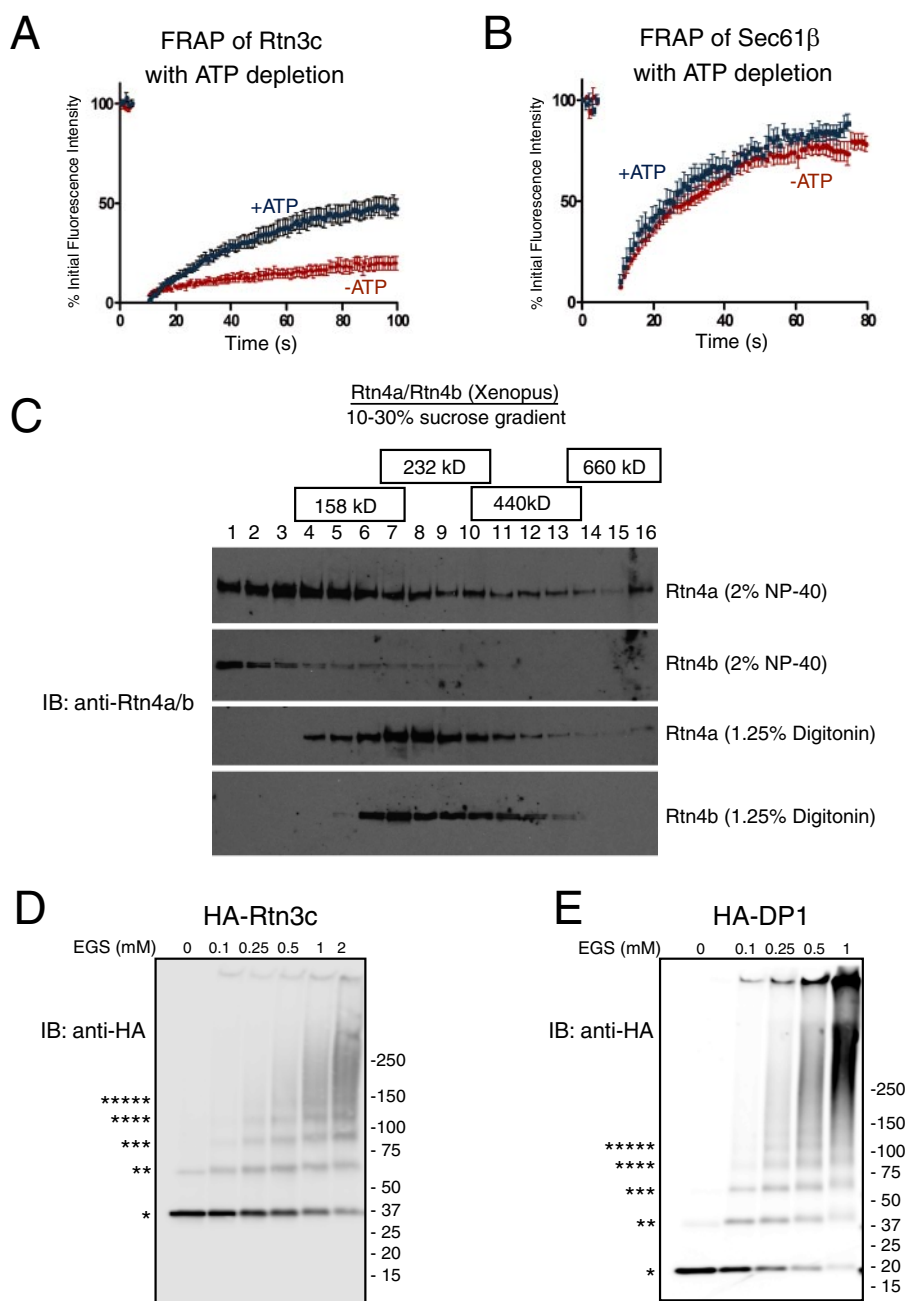


FIGURE 7. The reticulons and DP1 form oligomers in higher eukaryotes. *A*, quantitated FRAP analyses of mammalian GFP-Rtn3c under ATP-depleted (*red*, $n = 7$) or non-depleted (*blue*, $n = 14$) conditions. *B*, mammalian Sec61 β -GFP under ATP-depleted (*red*, $n = 9$) or non-depleted (*blue*, $n = 6$) conditions. FRAP data from ATP-depleted cells were compared with those from non-treated cells from Fig. 6. *C*, *Xenopus* membranes solubilized in either 1.25% digitonin or 2% Nonidet P-40 were fractionated by 10–30% w/v sucrose gradient centrifugation, analyzed by SDS-PAGE, and immunoblotted with antibody against *Xenopus* Rtn4. Molecular weight standards in the sucrose gradient are as indicated. *D*, isolated membranes of COS-7 cells expressing HA-DP1 or HA-Rtn3c were treated with increasing concentrations of EGS, analyzed on SDS-PAGE, and immunoblotted with anti-HA antibody. Asterisks, number of monomers cross-linked.

lian cells. This slow diffusion is probably not caused by their tethering to the cytoskeleton. Rather, immobility appears to be caused by their oligomerization that is evident in our sucrose gradient centrifugation and cross-linking experiments. The conserved RHD containing the two hydrophobic segments is sufficient for reticulon oligomerization; this domain alone causes slow lateral mobility in the membrane and forms homooligomers in cross-linking experiments. This conclusion is sup-

ported by the isolation of mutants of yeast Rtn1p that have amino acid changes in the RHD; they oligomerize less extensively according to sucrose gradient sedimentation experiments, and they diffuse rapidly in the membrane. The same mutants also no longer localize exclusively to the tubular ER, suggesting that oligomerization of the reticulons and DP1/Yop1p is required for their proper localization. We presume that oligomerization is also required for the ability of the reticulons and DP1/Yop1p to shape the tubular ER. In support of this notion, we found that the overexpression of the mammalian reticulons and DP1 stabilized ER tubules that would normally collapse in the absence of microtubules. However, oligomerization may not be sufficient, because Rtn1p mutant 91, which is defective in forming ER tubules, still shows oligomers in cross-linking experiments (data not shown).

How oligomerization causes the reticulons and DP1/Yop1p to localize to and induce the tubular ER is not yet clear, but other proteins that shape membranes into tubules also oligomerize. Examples include the caveolins that coat caveolae, flask-like invaginations at the plasma membrane, the EHD and PCH proteins that are involved in endocytosis, and the dynamins and dynamin-like proteins, GTPases that participate in vesicle budding and in shaping mitochondria (27–31). These proteins all oligomerize, and many are known to form spirals around membranes. Based on these precedents, one may speculate that the reticulons and DP1/Yop1p would use their propensity to oligomerize in a similar manner. However, the majority of the oligomers detected by sucrose density gradients and cross-linking experiments contained only four or five monomers, which would be insufficient to form a spiral around a membrane tubule. Our data do not exclude that larger oligomers are actually present *in vivo*, because they may dissociate upon solubilization in detergent and may not be detectable by cross-linking experiments. However, smaller oligomers could still shape tubules if they formed arc-like structures around the tubule. These arc-like oligomers could deform the lipid bilayer into tubules. Arc-shaped

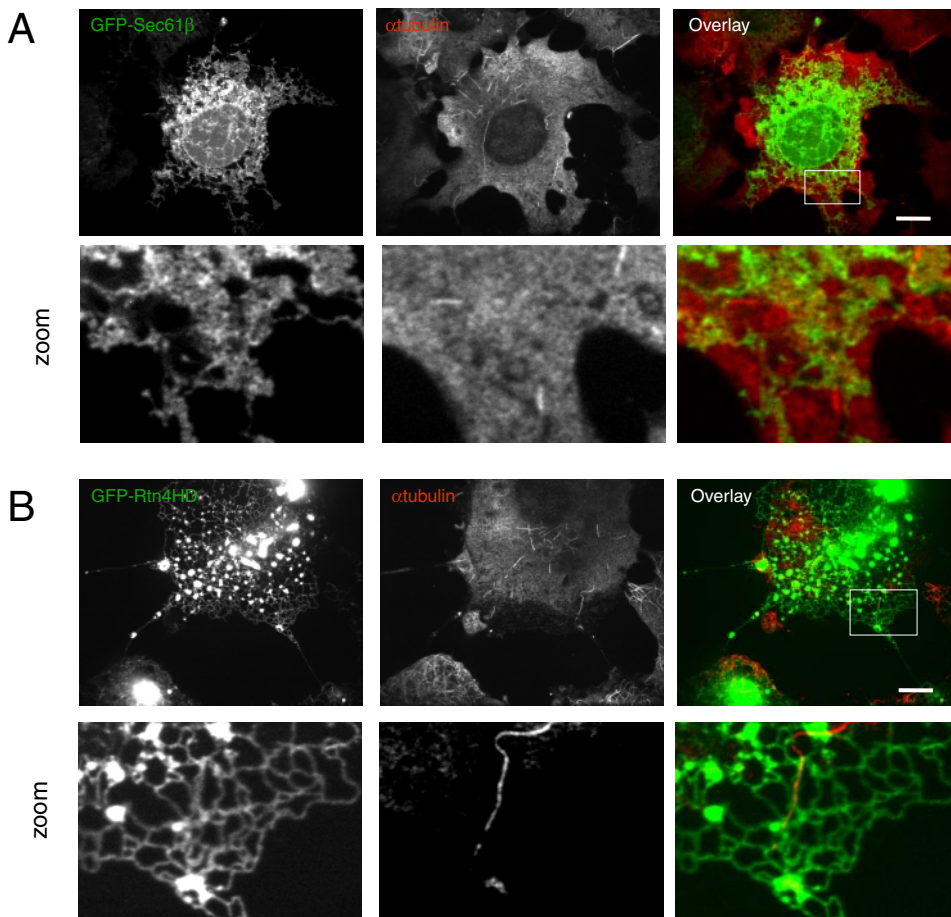


FIGURE 8. Overexpression of a reticulon stabilizes the tubular ER in the absence of microtubules in mammalian cells. *A*, a typical COS-7 cell expressing GFP-Sec61 β (green), where microtubules have been depolymerized by nocodazole treatment (immunostained with anti- α -tubulin, red), has collapsed, sheet-like peripheral ER. The lower row of panels shows an enlargement of the boxed region from the top panels. *B*, a typical COS-7 cell expressing GFP-Rtn3c (green) after microtubule depolymerization (stained in red) leads to an accumulation of bright foci containing Rtn3c but also retains much more tubular ER. The lower row of panels shows an enlargement of the boxed region from the top panels. Scale bar, 10 μ m.

oligomers may explain why relatively small oligomers of the reticulons and DP1/Yop1p may still diffuse slowly in the membrane: such structures would diffuse in a one-dimensional way along the tubule and would be hindered to pass one another or do so only very slowly. By contrast, globular particles of similar mass would diffuse much faster, because they can move two-dimensionally and would not be obstructed by one another. Finally, arc-shaped oligomers may also explain the localization of reticulons and DP1/Yop1p; it may be energetically most favorable for arcs to be in curved structures such as tubules. We propose that the reticulons and DP1/Yop1p not only form arc-like scaffolds around membrane tubules, but also use their central domain, including the two hydrophobic segments, to form a wedge-like structure in the membrane. The use of both “wedging” and “scaffolding” mechanisms would be analogous to how other proteins generate high curvature in membranes. For example, N-BAR domains wedge a hydrophobic segment into the outer leaflet of the lipid bilayer and form banana-shaped scaffolds (32).

We discovered that the diffusional mobilities of the reticulons and DP1 decrease upon ATP depletion. This finding suggests that the oligomers continuously form and disassemble *in vivo*, with the disassembly requiring ATP. Surprisingly, how-

ever, ATP depletion did not increase the size of the Rtn1-GFP oligomers in sucrose density gradient or cross-linking experiments (data not shown). Although it is therefore possible that ATP depletion affects the diffusion of the reticulons and DP1 in other ways, it is tempting to speculate that the dynamic nature of the oligomers would allow them to continuously form and disassemble at discrete but random sites throughout the ER. They could thus tubulate a larger surface of the ER than they physically occupy at any given moment. In fact, although the reticulons and DP1/Yop1p are some of the most abundant membrane proteins in the ER, they are not present in amounts that would allow them to cover the entire surface of all ER tubules. The postulated arc shape of the oligomers and their spacing on the tubules would allow other ER proteins to freely diffuse in the membrane.

It is also possible that an energy-driven disassembly is not the only mechanism by which the size of reticulon and DP1/Yop1p oligomers is restricted. We have found that homo-oligomers of these proteins tend to be larger than hetero-oligomers. Homo-oligomerization may therefore lead to excessive

amounts of these proteins in a given tubule. Because high concentrations of the reticulons and DP1/Yop1p have been shown to decrease the diameter of the tubule and displace resident luminal proteins (11, 33), different hetero-oligomeric combinations of the reticulons and DP1/Yop1p and their various isoforms may further regulate ER tubule shape.

Regulation of reticulon oligomerization may have physiological consequences as well. It has recently been shown that overexpression of Rtn3c in mice leads to large SDS-resistant oligomers in neurons, and these mice exhibit neuropathies similar to that of Alzheimer disease (20). Although it is unclear whether these aggregates are present in the tubular ER, it is appealing to speculate that this pathology results from excessive and unregulated oligomerization of the reticulons.

Acknowledgments—We thank E. Geras-Raaka and M. Gershengorn for help and use of the Zeiss LSM 510 NLO laser scanning inverted microscope; the HMS Nikon Imaging Facility, the BIDMC Flow Cytometry Core Facility, and Maria Ericsson of the HMS EM facility for help with experiments; and R. Massol and D. Pellman's group for initial help with mammalian FRAP experiments.

REFERENCES

1. Staehelin, L. A. (1997) *Plant J.* **11**, 1151–1165
2. Baumann, O., and Walz, B. (2001) *Int. Rev. Cytol.* **205**, 149–214
3. Voeltz, G. K., Rolls, M. M., and Rapoport, T. A. (2002) *EMBO Rep.* **3**, 944–950
4. Estrada de Martin, P., Novick, P., and Ferro-Novick, S. (2005) *Biochem. Cell Biol.* **83**, 752–761
5. Shibata, Y., Voeltz, G. K., and Rapoport, T. A. (2006) *Cell* **126**, 435–439
6. Voeltz, G. K., Prinz, W. A., Shibata, Y., Rist, J. M., and Rapoport, T. A. (2006) *Cell* **124**, 573–586
7. De Craene, J. O., Coleman, J., Estrada de Martin, P., Pypaert, M., Anderson, S., Yates, J. R., 3rd, Ferro-Novick, S., and Novick, P. (2006) *Mol. Biol. Cell* **17**, 3009–3020
8. Wakefield, S., and Tear, G. (2006) *Cell Mol. Life Sci.* **63**, 2027–2038
9. Audhya, A., Desai, A., and Oegema, K. (2007) *J. Cell Biol.* **178**, 43–56
10. Kiseleva, E., Morozova, K. N., Voeltz, G. K., Allen, T. D., and Goldberg, M. W. (2007) *J. Struct. Biol.* **160**, 224–235
11. Tolley, N., Sparkes, I. A., Hunter, P. R., Craddock, C. P., Nuttall, J., Roberts, L. M., Hawes, C., Pedrazzini, E., and Frigerio, L. (2008) *Traffic* **9**, 94–102
12. Prinz, W. A., Grzyb, L., Veenhuis, M., Kahana, J. A., Silver, P. A., and Rapoport, T. A. (2000) *J. Cell Biol.* **150**, 461–474
13. Klopfenstein, D. R., Klumperman, J., Lustig, A., Kammerer, R. A., Oorschot, V., and Hauri, H. P. (2001) *J. Cell Biol.* **153**, 1287–1300
14. Rolls, M. M., Stein, P. A., Taylor, S. S., Ha, E., McKeon, F., and Rapoport, T. A. (1999) *J. Cell Biol.* **146**, 29–44
15. Görlich, D., and Rapoport, T. A. (1993) *Cell* **75**, 615–630
16. Voeltz, G. K., and Prinz, W. A. (2007) *Nat. Rev. Mol. Cell Biol.* **8**, 258–264
17. Lippincott-Schwartz, J., Snapp, E., and Kenworthy, A. (2001) *Nat. Rev. Mol. Cell Biol.* **2**, 444–456
18. Lippincott-Schwartz, J., Altan-Bonnet, N., and Patterson, G. H. (2003) *Nat. Cell Biol. Suppl.* S7–S14
19. Dodd, D. A., Niederoest, B., Bloechlinger, S., Dupuis, L., Loeffler, J. P., and Schwab, M. E. (2005) *J. Biol. Chem.* **280**, 12494–12502
20. Hu, X., Shi, Q., Zhou, X., He, W., Yi, H., Yin, X., Gearing, M., Levey, A., and Yan, R. (2007) *EMBO J.* **26**, 2755–2767
21. He, W., Shi, Q., Hu, X., and Yan, R. (2007) *J. Biol. Chem.* **282**, 29144–29151
22. Fehrenbacher, K. L., Davis, D., Wu, M., Boldogh, I., and Pon, L. A. (2002) *Mol. Biol. Cell* **13**, 854–865
23. Waterman-Storer, C. M., and Salmon, E. D. (1998) *Curr. Biol.* **8**, 798–806
24. Ellenberg, J., Siggia, E. D., Moreira, J. E., Smith, C. L., Presley, J. F., Worman, H. J., and Lippincott-Schwartz, J. (1997) *J. Cell Biol.* **138**, 1193–1206
25. Oertle, T., and Schwab, M. E. (2003) *Trends Cell Biol.* **13**, 187–194
26. Terasaki, M., Chen, L. B., and Fujiwara, K. (1986) *J. Cell Biol.* **103**, 1557–1568
27. Rothberg, K. G., Heuser, J. E., Donzell, W. C., Ying, Y. S., Glenney, J. R., and Anderson, R. G. (1992) *Cell* **68**, 673–682
28. Daumke, O., Lundmark, R., Vallis, Y., Martens, S., Butler, P. J., and McMahon, H. T. (2007) *Nature* **449**, 923–927
29. Shimada, A., Niwa, H., Tsujita, K., Suetsugu, S., Nitta, K., Hanawa-Suetsugu, K., Akasaka, R., Nishino, Y., Toyama, M., Chen, L., Liu, Z. J., Wang, B. C., Yamamoto, M., Terada, T., Miyazawa, A., Tanaka, A., Sugano, S., Shirouzu, M., Nagayama, K., Takenawa, T., and Yokoyama, S. (2007) *Cell* **129**, 761–772
30. Hinshaw, J. E. (1999) *Curr. Opin. Struct. Biol.* **9**, 260–267
31. Ingerman, E., Perkins, E. M., Marino, M., Mears, J. A., McCaffery, J. M., Hinshaw, J. E., and Nunnari, J. (2005) *J. Cell Biol.* **170**, 1021–1027
32. Gallop, J. L., Jao, C. C., Kent, H. M., Butler, P. J., Evans, P. R., Langen, R., and McMahon, H. T. (2006) *EMBO J.* **25**, 2898–2910
33. Hu, J., Shibata, Y., Voss, C., Shemesh, T., Li, Z., Coughlin, M., Kozlov, M. M., Rapoport, T. A., and Prinz, W. A. (2008) *Science* **319**, 1247–1250